Near Infrared Absorption of $CdSe_xTe_{1-x}$ Alloyed Quantum Dot Sensitized Solar Cells with More than 6% Efficiency and High Stability

Zhenxiao Pan, Ke Zhao, Jin Wang, Hua Zhang, Yaoyu Feng, and Xinhua Zhong*

State Key Laboratory of Bioreactor Engineering, Institute of Applied Chemistry, East China University of Science and Technology, Shanghai 200237, China

ABSTRACT $CdSe_{0.45}Te_{0.55}$ alloyed quantum dots (QDs) with excitonic absorption onset at 800 nm and particle size of 5.2 nm were prepared *via* a noninjection high-temperature pyrolysis route and used as a sensitizer in solar cells. A postsynthesis assembly approach with use of bifunctional linker molecule mercaptopropionic acid (MPA) capped water-soluble QDs, obtained *via ex situ* ligand exchange from the initial oil-dispersible QDs, was adopted for tethering QDs onto mesoporous TiO_2 film. With the combination of high loading of the QD sensitizer and intrinsic superior optoelectronic properties (wide absorption range, high conduction band edge, high chemical stability, *etc.*, relative to their constituents CdSe and CdTe) of the adopted $CdSe_{0.45}Te_{0.55}$ QD sensitizer, the resulting $CdSe_xTe_{1-x}$ alloyed QD-based solar cells exhibit a record conversion efficiency of 6.36% (J_{sc} = 19.35 mA/cm^2, V_{oc} = 0.571 V, FF = 0.575) under full 1 sun illumination, which is remarkably better than that of the reference CdSe and CdTe QD based ones. Furthermore, the solar cells with Cu_2S counter electrodes based on eletrodeposition of Cu on conductive glass show long-term (more than 500 h) stability.

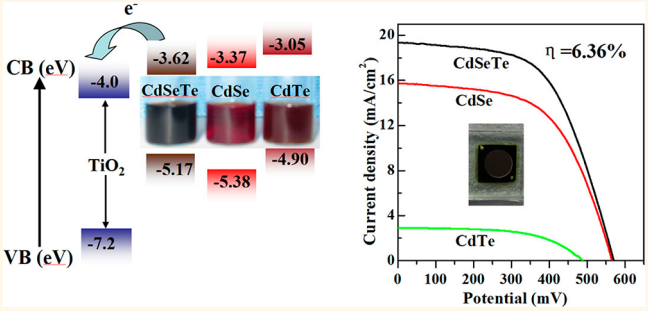

KEYWORDS: $CdSe_xTe_{1-x}$ · alloyed quantum dots · solar cells · high efficiency

Semiconductor quantum dot sensitized solar cells (QDSCs) constitute one of the most promising cost-effective candidates for third-generation photovoltaic cells due to the versatile advantages of QD sensitizers in comparison with conventional molecule dye sensitizers such as multiexciton generation, extraction of hot electrons, large intrinsic dipole moments, tunability of band gap, and high absorption coefficient.[1−7] However, at present, the recorded power conversion efficiency (PCE) values for liquid-junction QDSCs are typically below 6%,[8−14] remarkably lower than that of analogous dye-sensitized solar cells (11−12%),[15] partially because of the limitation of the light harvesting range of QD sensitizers, the low electron injection efficiency due to the unsatisfied conduction band edge relative to the metal oxide electron conductor (mainly TiO_2), and unsatisfactory surface coverage of QDs on mesoporous oxide film electrodes.[1−7] To obtain a high efficiency in QDSCs, ideal QD sensitizers should possess a narrow band gap (1.1−1.4 eV), a higher conduction band edge relative to that of TiO_2, and high stability.[1−7] Although utilization of QDs with large size and/or narrower band gap can expand the light harvesting range, large-sized QDs present a distinct disadvantage for penetrating into mesoporous oxide films, and the low conduction band edge of QDs prohibits effective injection of photoexcited electrons from the QD sensitizer into TiO_2. Therefore searching for suitable panchromatic QD sensitizers to expand the light harvesting range without hindering the subsequent electron extraction and ultimately obtaining a high PCE in the resulting cells is a great challenge.[1−7]

Initially, single binary QD sensitizers such as CdS, CdSe, PbS, PbSe, InP, and InAs were investigated in QDSCs, but most of these QDSCs presented low PCE values due to the limited light harvesting range and/or ineffectively photoexcited electron injection.[16−23]

* Address correspondence to zhongxh@ecust.edu.cn.

Received for review February 24, 2013 and accepted May 25, 2013.

Published online May 25, 2013
10.1021/nn400947e

In comparison, ternary or quaternary alloyed QDs are a promising alternative to binary QD sensitizers since their optoelectronic properties can be tuned by controlling their composition without changing the particle size,[24−26] and their band gap has the possibility to be narrower than their binary constituents due to an "optical bowing" effect.[27,28] Furthermore, alloyed QDs also show higher chemical stability than their constituents due to the hardened lattice structure and decreased interdiffusion.[29−31] To date, among the few attempts to explore alloyed QDs as sensitizers in liquid junction QDSCs,[32−36] the majority are focused on CdS_xSe_{1-x} alloyed QDs with a relative wide band gap.[35,36] Not surprisingly, this system did not exhibit a high PCE (<3%),[35,36] since the relatively short absorption edge wavelength (<700 nm) significantly limits the light harvesting range and thus results in a small photocurrent in the resulting cells. In comparison, $CdSe_xTe_{1-x}$ alloyed QDs with an absorption edge extending to the near-infrared (NIR) region should be a more attractive sensitizer.[37,38] To our best knowledge, there is only one report on the use of $CdSe_xTe_{1-x}$ alloyed QDs in solar cells, wherein a back contact depleted heterojunction device but not a liquid-junction-sensitized solar cell was constructed.[39]

Usually, two general approaches have been developed for tethering QDs onto TiO_2 electrodes: (i) direct growth of QDs onto a TiO_2 film; (ii) postsynthesis assembly using presynthesized QDs.[5,40] The first approach usually results in a very broad size distribution of the QD sensitizers, and the surface passivation of QDs is difficult to control, so that the electron transfer, charge recombination, and therefore the performance of the cell devices are detrimentally affected due to the uncontrolled optoelectronic features of the sensitizers.[40,41] These drawbacks can be effectively avoided by the second approach, using preprepared QDs, since the size, size distribution, shape, and surface functionalization, and consequently, the band gap alignment, optoelectronic properties, the density, and energy of the trap states of colloidal QDs, can be easily tailored and well controlled *via* the well-developed organometallic high-temperature synthetic method.[42] Furthermore, the shortcoming of low coverage of QDs on TiO_2 electrodes in the postsynthesis assembly approach has been effectively overcome recently by an *ex situ* ligand exchange route with use of bifunctional linker mercaptopropionic acid (MPA) capped water-soluble QDs or an electrophoretic deposition route.[8−10] As demonstrated in a previous report,[9] high surface coverage of QDs on a TiO_2 film (up to 34%) and uniform deposition along the whole film thickness were obtained *via* the postsynthesis assembly *ex situ* ligand exchange route, and a conversion efficiency of 5.4% was obtained in CdSe QD sensitized solar cells.

In this study a NIR absorption $CdSe_xTe_{1-x}$ alloy sensitizer was selected in the construction of high-efficiency QDSCs and compared with reference CdSe, CdTe QD based cells. High-quality NIR absorption $CdSe_{0.45}Te_{0.55}$ alloyed QDs were synthesized *via* a noninjection organometallic high-temperature protocol.[38] A postsynthesis assembly approach *ex situ* ligand exchange route with use of bifunctional linker MPA capped water-soluble QDs were adopted for depositing QD onto mesoporous TiO_2 film. With the combination of high loading of the QD sensitizer and intrinsic superior optoelectronic properties (wide absorption range, high conduction band edge, high chemical stability, *etc.*) of the adopted $CdSe_{0.45}Te_{0.55}$ QD sensitizer, the resulting solar cells exhibit a record PCE of 6.36% under full 1 sun illumination. Furthermore, the cells with Cu_2S counter electrodes based on electrodeposition of Cu on conductive glass show long-term (more than 500 h) stability.

RESULTS AND DISCUSSION

Superior Optoelectronic Properties. $CdSe_{0.45}Te_{0.55}$ alloyed QDs with a size of 5.2 ± 0.4 nm and an absorption edge at 800 nm (noted as $CdSeTe_{800}$ hereafter) were synthesized according to a literature method *via* a one-pot noninjection approach by heating a reaction mixture composed of cadmium oleate, TOP-Se (TOP, trioctylphosphine), and TOP-Te in paraffin media at 320 °C (detailed synthetic procedures are described in Materials and Methods, and characterization data are available in Figures S1 and S2 of the Supporting Information, SI).[38] It was noted that a vague band edge absorption feature appeared for the obtained $CdSe_{0.45}Te_{0.55}$ alloyed QDs, and thus an accurate band gap value was difficult to extract from the absorption spectrum. The band gap of 1.55 eV (800 nm) for $CdSe_{0.45}Te_{0.55}$ QDs is determined by plotting $(ah\nu)^2$ against the photon energy ($h\nu$), where a is the absorbance, h is Plank's constant, and ν is photon frequency (Figure S3). The adopted one-pot noninjection approach bears advantages of synthetic reproducibility and large-scale capability. For comparison, identical sized binary plain CdSe and CdTe QDs were also prepared according to developed protocols, and their corresponding absorption onsets were found to be 614 and 680 nm, respectively (noted as $CdSe_{614}$, $CdTe_{680}$).[43,44] The alloy structure of $CdSe_{0.45}Te_{0.55}$ QDs enables us to extend the absorption onset to the NIR window (800 nm), an unachievable target with either of the constituents. This is due to "optical bowing" effects in the alloyed structure associated with lattice mismatch between binary subcompounds and differences in atomic radii and electronegativities of the alloying elements.[28,29] NIR absorption of the obtained $CdSe_{0.45}Te_{0.55}$ QDs is an appealing property for their use as sensitizers in solar cells due to the wide light harvesting range and potentially high photocurrent in the resulting cells.[7]

Besides a narrower band gap, a suitable conduction band edge, which should be higher than that of TiO_2 in

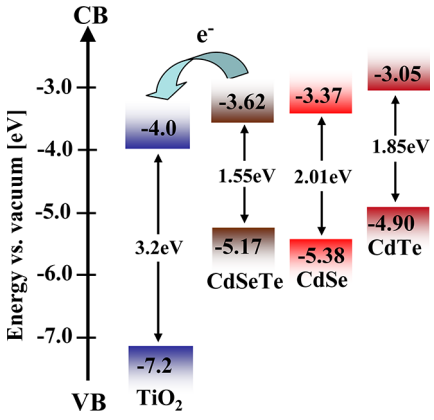

Figure 1. Schematic energy level diagram of TiO_2, $CdSeTe_{800}$, $CdSe_{614}$, and $CdTe_{680}$ QDs.

order to efficiently extract photogenerated electrons, is also critical for sensitizers in achieving high efficiency in the resulting cell devices.[1−7] To determine the effectiveness of $CdSeTe_{800}$ QDs serving as a sensitizer, it is vital to know the energy level diagram of the QDs. Thanks to the pioneering works by Jasieniak and coworkers,[39,45] the energy level diagrams of $CdSe_xTe_{1-x}$ alloy with varying composition and different sized binary QDs have been determined through the use of photoelectron spectroscopy in air. Therefore, the energy level diagram of $CdSeTe_{800}$ QDs together with references $CdSe_{614}$ and $CdTe_{680}$ QDs are schematically illustrated in Figure 1 based on the literature data.[39,45] According to ref 39, the valence band edge energies of $CdSe_xTe_{1-x}$ alloy show a nearly linear relationship with the chemical composition. Therefore the valence band edge energy (−5.17 eV) of $CdSeTe_{800}$ in our case can be calculated on the basis of the data for the same sized $CdSe_{614}$ and $CdTe_{680}$ QDs (−5.38, −4.90 eV, respectively). It is noted that the optical conduction band edge energies and valence band edge energies for $CdSe_{614}$ and $CdTe_{680}$ QDs are calculated on the basis of a particle size of 5.2 nm.[45] The calculated optical band gap values (2.01 eV for $CdSe_{614}$, 1.85 eV for $CdTe_{680}$) are close to the experimentally determined first excitonic absorption onsets in the corresponding absorption spectra (Figure S1). From Figure 1, it is clear that the CB edge of $CdSeTe_{800}$ is nearly at the same level as that of $CdSe_{614}$ QDs and 0.47 eV higher than that of TiO_2. Therefore the high CB edge of $CdSeTe_{800}$ favors electron injection into TiO_2.

Deposition of QDs onto TiO_2 Electrodes. In order to efficiently tether QD sensitizers onto mesoporous TiO_2 films with high loading, the as-prepared oil-soluble QDs were first made water-soluble *via* ligand exchange.[46] The native oil-soluble long hydrocarbon chain capping ligands (mainly oleylamine herein) around the QD surface were replaced by the bifunctional hydrophilic MPA ligand during the ligand exchange process, and thus water-soluble MPA-capped QDs were obtained. Absorption spectra and corresponding photographs of an MPA-capped $CdSeTe_{800}$ aqueous solution together with reference samples of $CdSe_{614}$ and $CdTe_{680}$ aqueous solutions are shown in Figure 2a. No significant change was observed for all three samples before and after phase transfer. The obtained water-soluble MPA-capped QD sensitizers were then tethered onto TiO_2 films according to a literature method by pipetting QD aqueous solutions (with absorbance of 2.0 at absorption onset) onto the oxide matrix and maintained for 2 h.[8,9]

Figure 2b shows the absorption spectra of identically sized $CdSeTe_{800}$, $CdTe_{680}$, and $CdSe_{614}$ QD sensitized TiO_2 films with corresponding photographs of the modified films together with bare TiO_2 film in the inset. It was found that the spectral profiles of the colloidal QD aqueous solutions were maintained after deposition onto TiO_2 films, reflecting an unchanged particle size and no particle aggregation. These features cannot be achieved by direct growth of QDs onto TiO_2 films as reported in previous reports.[10−23] The absorption spectra of the $CdSeTe_{800}$, $CdTe_{680}$, and $CdSe_{614}$ QD sensitized films show absorption onsets at nearly the same positions, around 800, 680, and 614 nm, respectively, as those for corresponding colloidal solutions. The photographs of the sensitized TiO_2 films show the same colors as their corresponding solutions. The relatively high absorbance by these electrodes gives us intuitive information of high QD loading, which can also be visualized from the deep coloration of the electrodes in the inset of Figure 2b. Due to no distinctive absorption peak in the absorption spectra and no reported extinction coefficient for the $CdSe_xTe_{1-x}$ QDs, the exact coverage of $CdSeTe_{800}$ QDs around the TiO_2 film cannot be calculated based on the absorption spectra of the sensitized film, but the high loading (34% coverage) and uniform distribution throughout the film based on this deposition method have been demonstrated in a previous report.[9] The black color of the $CdSeTe_{800}$-sensitized film indicates that the incident visible light can be absorbed nearly completely. Meanwhile the light harvesting range can be extended to wavelengths more than 800 nm. This paves the way for efficiently harvesting incident solar photons and high photocurrent in the resulting cell devices.

Cell Performance. After deposition of MPA-capped water-soluble QDs for 2 h, a thin passivation layer of ZnS was further deposited onto the sensitized TiO_2 films. Sandwich-type thin layer cells were fabricated by assembling the QD-sensitized TiO_2 film photoanode and Cu_2S on a brass foil counter electrode using binder clips. A polysulfide electrolyte was then filled (detailed procedure described in the Materials and Methods section). Similar to a previous report,[16] the $CdTe_{680}$ QD sensitizer was shown to suffer from chemical stability problems with a change of color from brown to pale while in contact with the electrolyte solution, and the photovoltaic performance of the corresponding

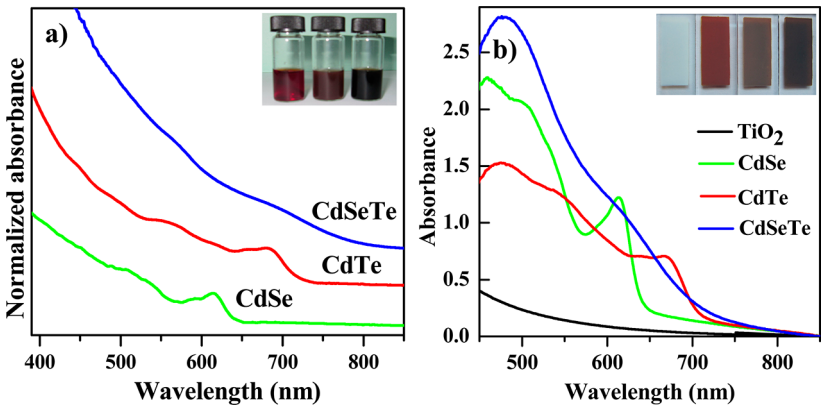

Figure 2. Absorption spectra of MPA-capped $CdSeTe_{800}$, $CdTe_{680}$, and $CdSe_{614}$ QD aqueous dispersions (a) and sensitized TiO_2 films (b). Insets: Photographs of $CdSeTe_{800}$, $CdTe_{680}$, and $CdSe_{614}$ QDs in turn from right to left.

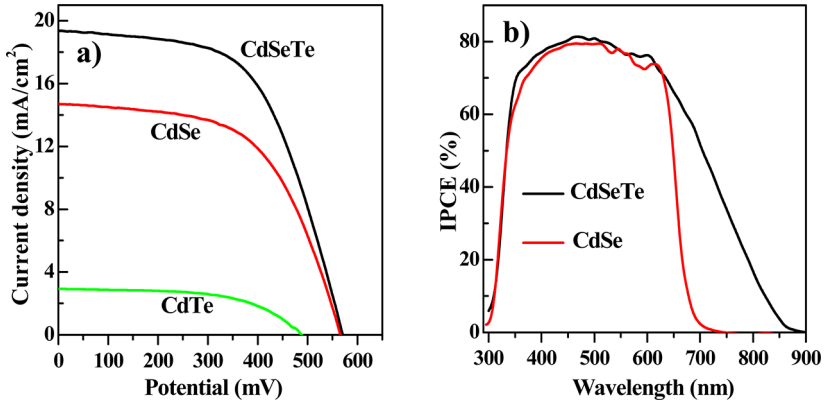

Figure 3. $J-V$ (a) and IPCE (b) curves of QDSCs based on different QD sensitizers.

TABLE 1. Photovoltaic Parameters Obtained from the $J-V$ Curves for Cells Based on Different QD Sensitizers with Identical Particle Size

QD	J_{sc} (mA/cm^2)	V_{oc} (mV)	FF (%)	η (%)
CdTe	2.92	487	0.573	0.81
CdSe	14.68	566	0.572	4.75
CdSeTe	19.35	571	0.575	6.36

cell device is quite poor (with a PCE of only 0.81%). The poor stability of the CdTe QD based solar cell is mainly because the sulfide/polysulfide electrolyte cannot scavenge holes from CdTe, thus resulting in degradation/oxidization of CdTe.[16] Therefore, no further characterization and discussions were performed on the CdTe-based cells. The $J-V$ curves of $CdSeTe_{800}$ and $CdSe_{614}$ cells under the illumination of AM 1.5 G at 1 full sun intensity (100 mW/cm^2) are shown in Figure 3a, and the main photovoltaic parameters are listed in Table 1. Both the fill factor (FF) and open voltage (V_{oc}) have no significant difference between the two cells, while the short-circuit current density (J_{sc}) for $CdSeTe_{800}$ (19.35 mA/cm^2) is remarkably greater than that of $CdSe_{614}$ (14.68 mA/cm^2). The higher photocurrent of $CdSeTe_{800}$ cells is mainly attributed to the extended light absorption range and the increase in absorptivity, as indicated by the corresponding absorption spectra shown in Figure 2. The similar fill factor implies analogous charge transfer resistance at the counter electrode/electrolyte interface since the electrocatalytic activity of the counter electrode with the electrolyte mainly affects the fill factor.[47,48] The photovoltage from a QDSC is not set by the QD band gap but rather set by the TiO_2 Fermi level offset from the redox potential of the electrolyte (polysulfide in our case). This can explain the V_{oc} values of the two cells being at the same level. The QDSCs based on $CdSe_{0.45}Te_{0.55}$ alloyed QD sensitizer exhibit the best performance, with J_{sc} = 19.35 mA/cm^2, V_{oc} = 0.571 V, FF = 0.575, and conversion efficiency (η) = 6.36%. The obtained 6.36% conversion efficiency is believed to be one of the highest values in the liquid-junction QDSCs so far.[8−23] It should be noted that the cell conversion efficiencies have a reduction of 4−5% when the methanol−water is replaced by regenerative water in the electrolytes. Other efforts to design all-solid-state bulk heterojunction quantum dot solar cells with Sb_2S_3, PbS, and PbI_2 have yielded PCEs in the range of 6−9%.[49−51]

The monochromatic incident-photon-to-carrier conversion efficiency (IPCE) spectra shown in Figure 3b

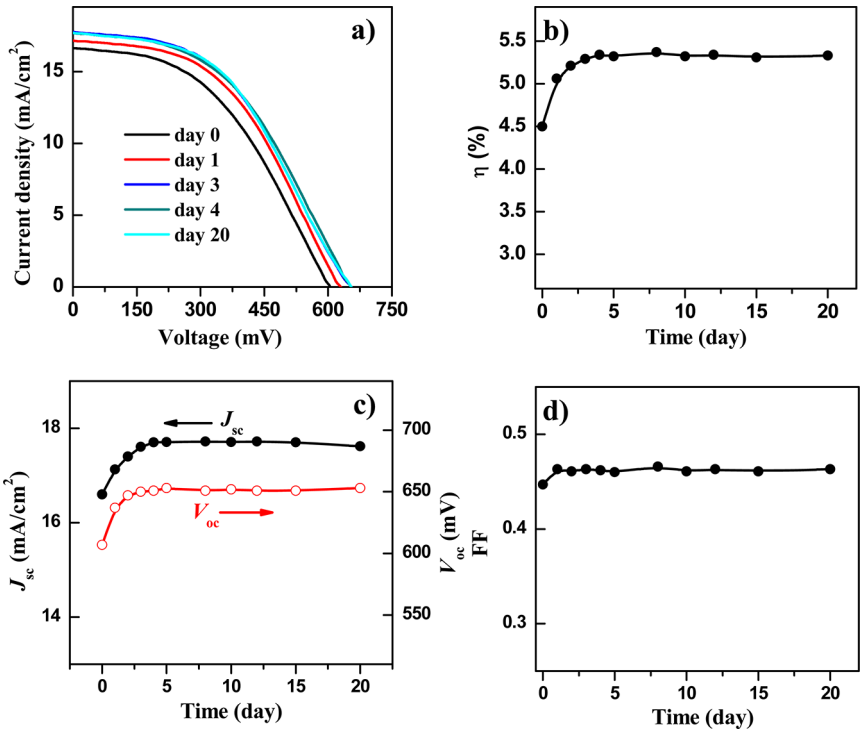

Figure 4. Temporal evolution of *J*−*V* curves (a) and photovoltaic parameter values, η (b), J_{sc}, V_{oc} (c), and FF (d), for the $CdSeTe_{800}$ cells based on Cu_2S counter electrodes *via* electrodeposition of Cu on FTO glass.

further verified the generation of a higher photocurrent in the $CdSeTe_{800}$-based cell devices. The overall photocurrent response matches the absorption features with photocurrent onsets around 650 nm for CdSe and 850 nm for CdSeTe cells. It should be noted that the photoresponse in IPCE spectra is wider in comparison with the absorption range in the absorption spectra. We think this is mainly due to the light-scattering effect by the large-sized TiO_2 particles (200−400 nm) in the scattering layer for IPCE measurement. This has been confirmed by the fact that the IPCE spectrum from the cells with scattering layers in the TiO_2 photoanodes displays a wider photoresponse range in comparison with that without scattering layers (Figure S4). IPCEs of ∼80% between 350 and 650 nm were achieved with both $CdSe_{614}$ and $CdSeTe_{800}$ sensitizers, but a much broader response wavelength region (from 350 to 850 nm) was found for the $CdSeTe_{800}$ sensitizer compared with only 350−650 nm for $CdSe_{614}$. This is consistent with the trend of J_{sc} values observed in the *J*−*V* characterization. This IPCE feature may be derived from the intrinsic electronic characteristics of a $CdSe_xTe_{1-x}$ alloyed structure sensitizer, as reflected in the absorption spectra. By integrating the product of the incident photon flux density and the cell's IPCE spectra,[52] the calculated J_{sc}'s for $CdSeTe_{800}$ and $CdSe_{614}$ cells are 18.02 and 13.39 mA/cm^2, respectively, which are quite close to the measured values shown in Table 1.

Cell Stability. Cell device stability is often overlooked but is critical to any real application. Prior research shows that QDSC devices with use of a Cu_2S counter electrode based on brass foil exhibit better performance.[8−26] The problem is that the brass foil substrate suffers from continual corrosion by the polysulfide electrolyte and thus leads to leakage of electrolyte solution. Our experimental results show that the electrolyte solution would dry up in such a cell device within 0.5 h, and the cell loses effectiveness ultimately. To overcome this shortcoming, the counter electrode was fabricated by electrodeposition of a ∼3 μm thick Cu film onto a FTO glass substrate that was subsequently immersed in polysulfide electrolyte solution for 15 min to form a Cu_2S/FTO counter electrode. Cells were constructed by sealing the counter electrode and the QD-sensitized FTO/TiO_2 photoanode using a thermoplastic spacer (noted as sealed cells hereafter). The stability of the sealed cells is remarkably improved, as can be seen in Figure 4, which shows temporal evolution of *J*−*V* curves and the extracted photovoltaic parameters (V_{oc}, J_{sc}, FF, and η included) values from *ex situ* long-term stability tests for more than 500 h, where the devices are stored in air at room light illumination without further encapsulation. The η value shows a steady increase of about 20% in the first 4 days, attaining a plateau thereafter. The improvement in η value is mainly contributed by the increase of V_{oc} and J_{sc} values. In contrast, the FF values remained nearly stable throughout. This is because the FF value is mainly determined by the counter electrode material. The fixation of FF value further demonstrates the long-term chemical and mechanical stability of the used counter electrode materials. The improvement in cell

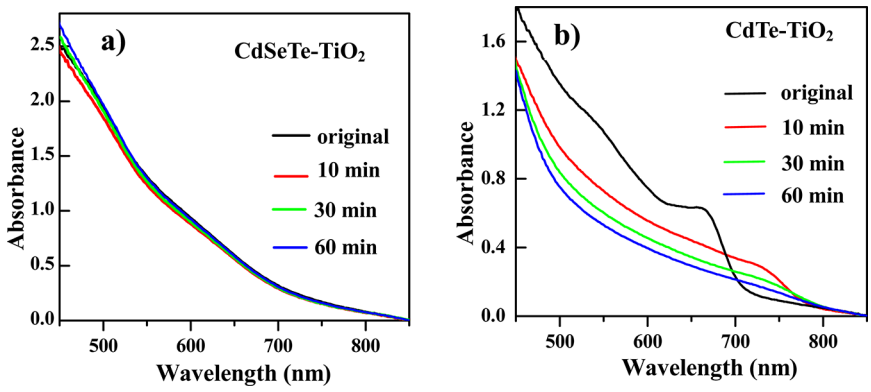

Figure 5. Temporal evolution of $CdSeTe_{800}$-TiO_2 (a) and $CdTe_{680}$-TiO_2 (b) films immersed in polysulfide electrolyte solution.

performance over time can be partially attributed to a capillary effect of slow electrolyte solution permeation into the TiO_2 pores.

The cell stability improvement is mainly benefited from the counter electrode materials prepared by electrodepositon of Cu on FTO glass, which prevents the diffusion of electrolyte solution out of the frame defined by the thermoplastic film. Furthermore, the chemical stability of the $CdSe_xTe_{1-x}$ alloyed QDs also favors the stability improvement of the cell device. We have qualitatively compared the stability of $CdSeTe_{800}$- and $CdTe_{680}$-sensitized TiO_2 films by means of absorption spectroscopy (Figure 5) when immersed into an electrolyte solution containing 2.0 M Na_2S, 2.0 M S, and 0.2 M KCl in methanol–water (3:7, v/v). In the case of the $CdSeTe_{800}$-TiO_2 film, the spectral changes are unobservable in the course of 1 h. In contrast, the $CdTe_{614}$-TiO_2 film shows a marked change, with an absorption feature finally resembling that of the TiO_2 film substrate. The spectral features indicate that there are no transformations for $CdSeTe_{800}$ QDs when immersed in a polysulfide electrolyte solution, while the CdTe QDs undergo complete decomposition. This highlights another possible benefit of using CdSeTe alloy over pure CdTe QDs.

CONCLUSIONS

In summary, being a sensitizer in QDSCs, $CdSe_xTe_{1-x}$ alloyed QDs are superior to their constituents CdSe and CdTe QDs and possess the advantage of a wider light harvesting range with absorption onset extending to the NIR region, higher chemical stability, and higher conduction band edge. With the combination of intrinsic superior optoelectronic properties of prepreared NIR absorping $CdSe_xTe_{1-x}$ alloyed QD sensitizers and effective deposition technique to ensure a high surface coverage of sensitizers, a conversion efficiency as high as 6.36% under simulated AM 1.5, full 1 sun illumination was obtained for the $CdSe_{0.45}Te_{0.55}$ QD based solar cells, which is one of the best results for liquid-junction QDSCs. The Cu_2S counter electrode based on electrodeposition of Cu on FTO glass can greatly improve the stability of the resulting cell devices.

MATERIALS AND METHODS

Materials. Cadmium oxide (CdO, 99.99%), selenium powder (99.99%), tellurium powder (200 mesh, 99.8%), oleyl amine (OAm), 1-octadecene (ODE, 90%), and trioctylphosphine (TOP, 90%) were purchased from Aldrich. Oleic acid (90%) and 1-tetradecylphosphonic acid (98%) were obtained from Alfa. Paraffin liquid (chemical grade) was purchased from Shanghai Chemical Reagents Company. All chemicals were used as received.

Synthesis of $CdSe_xTe_{1-x}$ Alloyed QDs. A literature method was adopted with minor modification.[38] Typically, 0.5 mL of 0.1 M Se and Te precursor solutions, prepared by dissolving Se or Te in TOP and paraffin (v/v, 1:3) at 60 or 250 °C under N_2, respectively, were mixed with 5.0 mL of 0.1 M Cd stock solution, obtained by dissolving CdO in oleic acid and paraffin (v/v, 1:3) at 200 °C under N_2 at room temperature in a three-neck flask clamped in a heating mantle with a Cd:Te:Se molar ratio of 10:1:1. Afterward, the resulting reaction mixture with a total volume of 6.0 mL was degassed at 110 °C for 10 min under vacuum to remove the moisture and oxygen. The reaction system was further heated to 320 °C at a rate of 10 °C/min under a N_2 atmosphere with vigorous stirring. After staying at 320 °C for 10 min, the reaction temperature was lowered to 260 °C, and 2.0 mL of OAm was added. The reaction system stayed at 260 °C for another 6 min before removing the heater and cooling to 60 °C. Then 10.0 mL of hexane–methanol (v/v, 1:1) was used as the extraction solvent to separate the nanocrystals from byproducts and unreacted precursors if present. The as-prepared $CdSe_xTe_{1-x}$ solution was further purified by centrifugation and decantation with the addition of acetone. $CdSe_xTe_{1-x}$ QDs with a particle size of 5.2 nm, absorption onset of 800 nm, and emission wavelength of 815 nm were obtained (noted as $CdSeTe_{800}$ hereafter). The optical spectra and corresponding TEM images of the obtained $CdSeTe_{800}$ QDs are shown in Figures S1 and S2 of the SI, respectively. The chemical composition of the obtained alloyed QDs is $CdSe_{0.45}Te_{0.55}$ based on inductively coupled plasma atomic emission spectroscopy (ICP-AES) measurement. Furthermore, 5.2 nm sized CdSe and CdTe QDs were synthesized using developed literature methods.[43,44]

Preparation of MPA-Capped Water-Soluble QDs. The water solubilization of the as-prepared oil-soluble QDs was obtained by replacing the initial hydrophobic surfactants (OAm and/or oleic acid) with mercaptopropionic acid according to a literature method.[46] Typically, MPA (0.212 g, 0.2 mmol) was dissolved in

0.3 mL of deionized water together with 1.0 mL of methanol, and the solution was then adjusted to pH 12 with 40% NaOH. The MPA–methanol solution was then added into 5.0 mL of $CdSe_xTe_{1-x}$ QDs chloroform solution (containing 0.2 mmol of QDs) and stirred for 30 min to precipitate the QDs. Then 10.0 mL of water was added into the mixture, and the stirring was continued for another 20 min. The solution was finally separated into two phases, the $CdSe_xTe_{1-x}$ QDs were transferred into the superincumbent water from the underlying chloroform, the underlying organic phase was discarded, and the aqueous phase containing the QDs was collected. The free MPA ligand in the QD aqueous solution was isolated by precipitating the QDs by the addition of acetone. The supernatant was discarded, and the pellet was then redissolved in water for use in the next step. The procedure for phase transfer of CdSe and CdTe is the same as that for CdSeTe QDs.

Fabrication and Photovoltaic Characterization of Solar Cells. TiO_2 nanoparticulate electrodes were prepared by successively screen printing an 11.0 μm thick transparent layer (P25 paste) and a 4.0 μm thick light-scattering layer (200–400 nm TiO_2) over F:SnO_2-coated (FTO, 14 Ω/square) glass substrates, followed by sintering at 450 °C for 30 min in a muffle-type furnace. A post-treatment of the dried TiO_2 film with an aqueous solution of $TiCl_4$ (0.04 M) was then carried out according to typical procedures for dye cells. The obtained TiO_2 mesoporous films were then coated with QDs sensitizers.

For immobilization of QDs, 30 μL of MAP-capped QDs aqueous solution (with an absorbance of 2.0 at the first excitonic absorption peak) was pipetted directly on the electrode surface, where it stayed for 2 h before rinsing sequentially with water and ethanol and then drying with nitrogen. After the deposition was complete, the QD absorbed TiO_2 film was coated with ZnS by twice dipping alternately into 0.1 M $Zn(OAc)_2$ and 0.1 M Na_2S aqueous solutions for 1 min/dip. The role of the deposited ZnS shell is to suppress the charge recombination at the QD sensitizer/electrolyte interface and thus to improve the PCE.[48]

The Cu_2S counter electrodes were prepared by immersing brass foil in a HCl solution at 70 °C for 5 min, and then the brass foil was vulcanized by injecting a polysulfide solution after solar cell fabrication. The polysulfide electrolyte solution consists of 2.0 M Na_2S, 2.0 M S, and 0.2 M KCl in a methanol–water (3:7, v/v) solution. The cells were prepared by assembling the counter electrode and a QD-sensitized photoanode using a 50 μm thick Scotch spacer with a binder clip. A droplet (10 μL) of polysulfide electrolyte was then added. For QDSCs prepared under each condition, three cells were prepared and tested in parallel, and the one with the medium value was chosen as the final data.

In the process of the stability test for sealed cells, the Cu_2S counter electrodes were prepared based on electrodeposition of Cu on FTO glass. Cu films with an area of 0.7 × 0.7 cm^2 were deposited on FTO glass by the multipotential steps technique using a Luggin capillary for a saturated calomel reference electrode (SCE) and a phosphorus copper as the counter electrode. The electrolytes for Cu electrodeposition consist of an aqueous solution of 9 mM Cu_2SO_4 and 5 mM H_2SO_4. The potential was normally scanned at −5 V for 0.2 s and then at 0 V for 0.4 s with 10 000 cycles. After deposition, the FTO electrode was immersed in polysulfide electrolyte solution for 15 min to generate Cu_2S.

The sealed cells used in the stability test were prepared by sealing the Cu_2S counter electrode based on electrodeposition of Cu on FTO and the QD-sensitized FTO/TiO_2 electrode using a thermoplastic spacer (DuPont Surlyn 1702, thickness 50 μm). The electrolyte (identical to that described above) was introduced into the sealed cell through a hole predrilled in the counter electrode, which was sealed after filling. This cell device is called a sealed cell.

Photovoltaic performances (J–V curves) of cell devices were recorded on a Keithley 2400 source meter under illumination by a AM 1.5 G solar simulator (Oriel, model no. 91160, equipped with a 150 W xenon lamp). The power of the simulated light was calibrated to 100 mW/cm^2 by an NREL standard Si solar cell. The photoactive area was 0.237 cm^2. The IPCE signal was recorded on a Keithley 2000 multimeter under the illumination of a 300 W tungsten lamp with a Spectral Products DK240 monochromator.

TEM Images and Optical Spectroscopy Characterization. Transition electron microscopy (TEM) images were obtained using a JEOL JEM-1400 instrument. The TEM samples were prepared by depositing a drop of QD dilute toluene solution onto copper grids with a carbon support and evaporating the solvent in air at room temperature. The absorption spectra of QD-sensitized electrodes composed of 11.0 μm thick TiO_2 films with dimensions of 2.0 × 1.0 cm (without scattering layers) were recorded on a UV–visible spectrophotometer (Shimadzu UV-2450). The steady-state photoluminescence (PL) emission spectra were recorded on a Cary Eclipse (Varian) fluorescence spectrophotometer. The composition for the $CdSe_xTe_{1-x}$ QDs was measured by means of ICP-AES (Thermo Elemental IRIS 1000) using HCl–HNO_3 digestion.

Conflict of Interest: The authors declare no competing financial interest.

Acknowledgment. This work has been financially supported by National Natural Science Foundation of China (No. 21175043), the Science and Technology Commission of Shanghai Municipality (11JC1403100, 12ZR1407700), the National Special Fund for State Key Laboratory of Bioreactor Engineering (No. 2060204), and the Fundamental Research Funds for the Central Universities.

Supporting Information Available: Optical and TEM characterization of the $CdSe_{0.45}Te_{0.55}$, $CdSe_{614}$, and $CdTe_{680}$ QD sensitizers. This material is available free of charge *via* the Internet at http://pubs.acs.org.

REFERENCES AND NOTES

1. Kamat, P. V. Quantum Dot Solar Cells. Semiconductor Nanocrystals as Light Harvesters. *J. Phys. Chem. C* **2008**, *112*, 18737–18753.
2. Ruhle, S.; Shalom, M.; Zaban, A. Quantum-Dot-Sensitized Solar Cells. *ChemPhysChem* **2010**, *11*, 2290–2304.
3. Kamat, P. V.; Tvrdy, K.; Baker, D. R.; Radich, J. G. Beyond Photovoltaics: Semiconductor Nanoarchitectures for Liquid-Junction Solar Cells. *Chem. Rev.* **2010**, *110*, 6664–6688.
4. Kamat, P. V. Boosting the Efficiency of Quantum Dot Sensitized Solar Cells through Modulation of Interfacial Charge Transfer. *Acc. Chem. Res.* **2012**, *45*, 1906–1915.
5. Yang, Z.; Chen, C.-Y.; Liu, C.-W.; Chang, H.-T. Electrocatalytic Sulfur Electrodes for CdS/CdSe Quantum Dot-Sensitized Solar Cells. *Chem. Commun.* **2010**, *46*, 5485–5487.
6. Hetsch, F.; Xu, X.; Wang, H.; Kershaw, S. V.; Rogach, A. L. Semiconductor Nanocrystal Quantum Dots as Solar Cell Components and Photosensitizers: Material, Charge Transfer, and Separation Aspects of Some Device Topologies. *J. Phys. Chem. Lett.* **2011**, *2*, 1879–1887.
7. Mora-Sero, I.; Bisquert, J. Breakthroughs in the Development of Semiconductor-Sensitized Solar Cells. *J. Phys. Chem. Lett.* **2010**, *1*, 3046–3052.
8. Pan, Z.; Zhang, H.; Cheng, K.; Hou, Y.; Hua, J.; Zhong, X. Highly Efficient Inverted Type-I CdS/CdSe Core/Shell Structure QD-Sensitized Solar Cells. *ACS Nano* **2012**, *6*, 3982–3991.
9. Zhang, H.; Cheng, K.; Hou, Y.; Fang, Z.; Pan, Z.; Wu, W.; Hua, J.; Zhong, X. Efficient CdSe Quantum Dot-Sensitized Solar Cells Prepared by a Postsynthesis Assembly Approach. *Chem. Commun.* **2012**, *48*, 11235–11237.
10. Yu, X.; Liao, J.; Qiu, K.; Kuang, D.; Su, C. Dynamic Study of Highly Efficient CdS/CdSe Quantum Dot Sensitized Solar Cells Fabricated by Electrodeposition. *ACS Nano* **2011**, *5*, 9494–9500.
11. Santra, P. K.; Kamat, P. V. Mn-Doped Quantum Dot Sensitized Solar Cells: A Strategy to Boost Efficiency over 5%. *J. Am. Chem. Soc.* **2012**, *134*, 2508–2511.
12. Hossain, Md. A.; Jennings, J. R.; Shen, C.; Pan, J. H.; Koh, Z. Y.; Mathews, N.; Wang, Q. CdSe-Sensitized Mesoscopic TiO_2 Solar Cells Exhibiting > 5% Efficiency: Redundancy of CdS Buffer Layer. *J. Mater. Chem.* **2012**, *22*, 16235–16242.
13. Zhang, Q.; Guo, X.; Huang, X.; Huang, S.; Li, D.; Luo, Y.; Shen, Q.; Toyoda, T.; Meng, Q. Highly Efficient CdS/CdSe-Sensitized Solar Cells Controlled by the Structural Properties of

Compact Porous TiO_2 Photoelectrodes. *Phys. Chem. Chem. Phys.* **2011**, *13*, 4659–4667.
14. Im, J.-H.; Lee, C.-R.; Lee, J.-W.; Park, S.-W.; Park, N.-G. 6.5% Efficient Perovskite Quantum-Dot-Sensitized Solar Cell. *Nanoscale* **2011**, *3*, 4088–4093.
15. Hagfeldt, A.; Boschloo, G.; Sun, L.; Kloo, L.; Pettersson, H. Dye-Sensitized Solar Cells. *Chem. Rev.* **2010**, *110*, 6595–6663.
16. Bang, J. H.; Kamat, P. V. Quantum Dot Sensitized Solar Cells. A Tale of Two Semiconductor Nanocrystals: CdSe and CdTe. *ACS Nano* **2009**, *3*, 1467–1476.
17. Wang, H.; Luan, C.; Xu, X.; Kershaw, S. V.; Rogach, A. L. In Situ versus ex Situ Assembly of Aqueous-Based Thioacid Capped CdSe Nanocrystals within Mesoporous TiO_2 Films for Quantum Dot Sensitized Solar Cells. *J. Phys. Chem. C* **2012**, *116*, 484–489.
18. Kongkanand, A.; Tvrdy, K.; Takechi, K.; Kuno, M.; Kamat, P. V. Quantum Dot Solar Cells. Tuning Photoresponse through Size and Shape Control of CdSe-TiO_2 Architecture. *J. Am. Chem. Soc.* **2008**, *130*, 4007–4015.
19. Lee, H. J.; Chen, P.; Moon, S. J.; Sauvage, F.; Sivula, K.; Bessho, T.; Gamelin, D. R.; Comte, P.; Zakeeruddin, S. M.; Seok, S. I.; *et al*. Regenerative PbS and CdS Quantum Dot Sensitized Solar Cells with a Cobalt Complex as Hole Mediator. *Langmuir* **2009**, *25*, 7602–7608.
20. Yu, P. R.; Zhu, K.; Norman, A. G.; Ferrere, S.; Frank, A. J.; Nozik, A. J. Nanocrystalline TiO_2 Solar Cells Sensitized with InAs Quantum Dots. *J. Phys. Chem. B* **2006**, *110*, 25451–25454.
21. Luan, C.; Vaneski, A.; Susha, A. S.; Xu, X.; Wang, H.-E.; Chen, X.; Xu, J.; Zhang, W.; Lee, C.-S.; Rogach, A. L. Facile Solution Growth of Vertically Aligned ZnO Nanorods Sensitized with Aqueous CdS and CdSe Quantum Dots for Photovoltaic Applications. *Nanoscale Res. Lett.* **2011**, *6*, 340.
22. Liu, L.; Hensel, J.; Fitzmorris, R. C.; Li, Y.; Zhang, J. Z. Preparation and Photoelectrochemical Properties of CdSe/TiO_2 Hybrid Mesoporous Structures. *J. Phys. Chem. Lett.* **2010**, *1*, 155–160.
23. Laghumavarapu, R. B.; El-Emawy, M.; Nuntawong, N.; Moscho, A.; Lester, L. F.; Huffaker, D. L. Improved Device Performance of InAs/GaAs Quantum Dot Solar Cells with GaP Strain Compensation Layers. *Appl. Phys. Lett.* **2007**, *91*, 243115.
24. Smith, A. M.; Nie, S. Semiconductor Nanocrystals: Structure, Properties, and Band Gap Engineering. *Acc. Chem. Res.* **2010**, *43*, 190–200.
25. Regulacio, M. D.; Han, M.-Y. Composition-Tunable Alloyed Semiconductor Nanocrystals. *Acc. Chem. Res.* **2010**, *43*, 621–630.
26. Peng, X. Band Gap and Composition Engineering on a Nanocrystal (BCEN) in Solution. *Acc. Chem. Res.* **2010**, *43*, 1387–1395.
27. Bernard, J. E.; Zunger, A. Electronic Structure of ZnS, ZnSe, ZnTe, and Their Pseudobinary Alloys. *Phys. Rev. B* **1987**, *36*, 3199–3228.
28. Feng, Z. C.; Becla, P.; Kim, L. S.; Perkowitz, S.; Feng, Y. P.; Poon, H. C.; Williams, K. P.; Pitt, G. D. Raman, Infrared, Photoluminescence and Theoretical Studies of the II-VI-VI Ternary CdSeTe. *J. Cryst. Growth* **1994**, *138*, 239–243.
29. Bell, S. L.; Sen, S. J. Crystal Growth of $Cd_{1-x}Zn_xTe$ and Its Use as a Superior Substrate for LPE Growth of $Hg_{0.8}Cd_{0.2}Te$. *Vac. Sci. Technol.* **1985**, *A3*, 112–115.
30. Zhong, X.; Han, M.; Dong, Z.; White, T. J.; Knoll, W. Composition-Tunable $Zn_xCd_{1-x}Se$ Nanocrystals with High Luminescence and Stability. *J. Am. Chem. Soc.* **2003**, *125*, 8589–8594.
31. Zhong, X.; Feng, Y.; Knoll, W.; Han, M. Alloyed $Zn_xCd_{1-x}S$ Nanocrystals with Highly Narrow Luminescence Spectral Width. *J. Am. Chem. Soc.* **2003**, *125*, 13559–13563.
32. Xu, J.; Yang, X.; Wang, H.; Chen, X.; Luan, C.; Xu, Z.; Lu, Z.; Roy, V. A. L.; Zhang, W.; Lee, C.-S. Arrays of ZnO/$Zn_xCd_{1-x}Se$ Nanocables: Band Gap Engineering and Photovoltaic Applications. *Nano Lett.* **2012**, *11*, 4138–4143.
33. Ma, W.; Luther, J. M.; Zheng, H.; Wu, Y.; Alivisatos, A. P. Photovoltaic Devices Employing Ternary PbS_xSe_{1-x} Nanocrystals. *Nano Lett.* **2009**, *9*, 1699–1703.
34. McDaniel, H.; Fuke, N.; Pietryga, J. M.; Klimov, V. I. Engineered $CuInSe_xS_{2-x}$ Quantum Dots for Sensitized Solar Cells. *J. Phys. Chem. Lett.* **2013**, *4*, 355–361.
35. Shu, T.; Zhou, Z.; Wang, H.; Liu, G.; Xiang, P.; Rong, Y.; Han, H.; Zhao, Y. Efficient Quantum Dot-Sensitized Solar Cell with a Tunable Energy Band $CdSe_xS_{(1-x)}$ Quantum Dot. *J. Mater. Chem.* **2012**, *22*, 10525–10529.
36. Santra, P. K.; Kamat, P. V. Tandem-Layered Quantum Dot Solar Cells: Tuning the Photovoltaic Response with Luminescent Ternary Cadmium Chalcogenides. *J. Am. Chem. Soc.* **2013**, *135*, 877–885.
37. Bailey, R. E.; Nie, S. Alloyed Semiconductor Quantum Dots: Tuning the Optical Properties without Changing the Particle Size. *J. Am. Chem. Soc.* **2003**, *125*, 7100–7106.
38. Liao, L.; Zhang, H.; Zhong, X. Facile Synthesis of Red-to Near-Infrared-Emitting $CdTe_xSe_{1-x}$ Alloyed Quantum Dots *via* a Noninjection One-Pot Route. *J. Lumin.* **2011**, *131*, 322–327.
39. MacDonald, B. I.; Martucci, A.; Rubanov, S.; Watkins, S. E.; Mulvaney, P.; Jasieniak, J. J. Layer-by-Layer Assembly of Sintered $CdSe_xTe_{1-x}$ Nanocrystal Solar Cells. *ACS Nano* **2012**, *6*, 5995–6004.
40. Mora-Sero, I.; Gimenez, S.; Fabregat-Santiago, F.; Gomez, R.; Shen, Q.; Toyota, T.; Bisquert, J. Recombination in Quantum Dot Sensitized Solar Cells. *Acc. Chem. Res.* **2009**, *42*, 1848–1857.
41. Hodes, G. Comparison of Dye- and Semiconductor-Sensitized Porous Nanocrystalline Liquid Junction Solar Cells. *J. Phys. Chem. C* **2008**, *112*, 17778–17787.
42. Watson, D. F. Linker-Assisted Assembly and Interfacial Electron-Transfer Reactivity of Quantum Dot−Substrate Architectures. *J. Phys. Chem. Lett.* **2010**, *1*, 2299–2309.
43. Zhong, X.; Feng, Y.; Zhang, Y. Facile and Reproducible Synthesis of Red-Emitting CdSe Nanocrystals in Amine with Long-Term Fixation of Particle Size and Size Distribution. *J. Phys. Chem. C* **2007**, *111*, 526–531.
44. Yu, W. W.; Wang, A.; Peng, X. G. Formation and Stability of Size-, Shape-, and Structure-Controlled CdTe Nanocrystals: Ligand Effects on Monomers and Nanocrystals. *Chem. Mater.* **2003**, *15*, 4300–4308.
45. Jasieniak, J.; Califano, M.; Watkins, S. E. Size-Dependent Valence and Conduction Band-Edge Energies of Semiconductor Nanocrystals. *ACS Nano* **2011**, *5*, 5888–5902.
46. Liu, L.; Guo, X.; Li, Y.; Zhong, X. Bifunctional Multidentate Ligand Modified Highly Stable Water-Soluble Quantum Dots. *Inorg. Chem.* **2010**, *49*, 3768–3775.
47. Fabregat-Santiago, F.; Garcia-Belmonte, G.; Mora-Sero, I.; Bisquert, J. Characterization of Nanostructured Hybrid and Organic Solar Cells by Impedance Spectroscopy. *Phys. Chem. Chem. Phys.* **2011**, *13*, 9083–9118.
48. Gimenez, S.; Mora-Sero, I.; MacOr, L.; Guijarro, N.; Lana-Villarreal, T.; Gomez, R.; Diguna, L. J.; Shen, Q.; Toyoda, T.; Bisquert, J. Improving the Performance of Colloidal Quantum-Dot-Sensitized Solar Cells. *Nanotechnology* **2009**, *20*, 295204.
49. Im, S. H.; Lim, C.-S.; Chang, J. A.; Lee, Y. H.; Maiti, N.; Kim, H.-J.; Nazeeruddin, Md. K.; Gratzel, M.; Seok, S. I. Toward Interaction of Sensitizer and Functional Moieties in Hole-Transporting Materials for Efficient Semiconductor-Sensitized Solar Cells. *Nano Lett.* **2011**, *11*, 4789–4793.
50. Ip, A. H.; Thon, S. M.; Hoogland, S.; Voznyy, O.; Zhitomirsky, D.; Debnath, R.; Levina, L.; Rollny, L. R.; Carey, G. H.; Fischer, A.; *et al*. Hybrid Passivated Colloidal Quantum Dot Solids. *Nat. Nanotechnol.* **2012**, *7*, 577–582.
51. Kim, H.-S.; Lee, C.-R.; Im, J.-H.; Lee, K.-B.; Moehl, T.; Marchioro, A.; Moon, S.-J.; Humphry-Baker, R.; Yum, J.-H.; Moser, J. E.; *et al*. Lead Iodide Perovskite Sensitized All-Solid-State Submicron Thin Film Mesoscopic Solar Cell with Efficiency Exceeding 9%. *Sci. Rep.* **2012**, *2*, 591.
52. Tachibana, Y.; Hara, K.; Sayama, K.; Arakawa, H. Quantitative Analysis of Light-Harvesting Efficiency and Electron-Transfer Yield in Ruthenium-Dye-Sensitized Nanocrystalline TiO_2 Solar Cells. *Chem. Mater.* **2002**, *14*, 2527–2535.